Environmental Science Nano

ROYAL SOCIETY OF CHEMISTRY

PAPER

View Article Online
View Journal | View Issue

Check for updates

Cite this: *Environ. Sci.: Nano*, 2022, **9**, 4484

Ceramic fibers do not exhibit larger toxicity in pulmonary epithelial cells than nanoparticles of the same chemical composition†

Jana Bacova, [a] Ludek Hromadko, [bc] Pavlina Nyvltová, [a] Lenka Bruckova, [a] Martin Motola, ‡[b] Roman Bulanek, [d] Martina Rihova, [bc] Tomas Rousar *[a] and Jan M. Macak *[bc]

Received 9th March 2022,
Accepted 8th October 2022

DOI: 10.1039/d2en00217e

rsc.li/es-nano

Herein, the first comprehensive toxicity study of Al_2O_3, SiO_2, ZrO_2, TiO_2 and WO_3 fiber effects in cultured epithelial A549 cells is presented. The fibers were produced by centrifugal spinning from suitable spinning solutions and have an average diameter in the sub-micrometer range. At first, we characterized the fibers for their morphological, compositional and structural properties. Then, we estimated the biological effects of fibers in pulmonary epithelial A549 cells comparing them with the biological effects of Al_2O_3, SiO_2, ZrO_2, TiO_2 and WO_3 nanoparticles. Multiwalled carbon nanotubes (MWCNTs) were used as a positive control. The cells were treated with 1, 10 and 100 μg mL^{-1} concentrations of a nanomaterial for 24 and 48 h. The dehydrogenase activity and glutathione levels were determined in cells as markers of cell injury. We found that the tested fibers exhibited no deleterious effects in A549 cells except for Al_2O_3 and TiO_2 fibers causing significant cell damage of similar extent to Al_2O_3 and TiO_2 nanoparticles, respectively. Overall, we conclude that the herein tested inorganic fibers do not exhibit larger toxicity risk in human pulmonary A549 cells in comparison to nanoparticles of the same chemical composition.

Environmental significance

The development and production of nanomaterials has been increasing in recent years around the world. Nanomaterials provide unique physical, chemical and biological properties that enable their use in various fields of human beings. They also show potential for many emerging environmental applications. New technologies enable synthesis of innovative nanomaterials, including nanofibers of unique composition. Although the use of nanofibers has been increasing, the lack of elucidation of biological effects after potential environmental exposure of humans remains. Due to inhalation from the environment, possibly leading to changes in pulmonary cells, any toxicity studies on nanofibers effects in lung cells are of large significance. Thus, we present here for the first time a study on biological effects of nanofibers in lung cells and we compare the results to inorganic nanoparticles of the same composition.

Introduction

Development and production of various nanomaterials have been ever increasing in recent years. Nanomaterials include a diverse group of various inorganic, organic and hybrid structures that have at least one dimension on the nanoscale (by definition of ISO/TS 80004 ≤ 100 nm). All these materials possess unique physical, chemical and biological properties that enable their use in various fields, such as (photo) electrochemistry, electronics, cosmetics, and medicine and they also exhibit exquisite potential for many emerging environmental applications.[1–6]

While significant attention has been devoted to the development and application of new nanomaterials, considerably less attention has been given to the study of their diverse biological effects. Thus, it is important to

[a] *Department of Biological and Biochemical Sciences, Faculty of Chemical Technology, University of Pardubice, Studentska 573, 532 10 Pardubice, Czech Republic. E-mail: Tomas.Rousar@upce.cz; Tel: +420 466 037 707*
[b] *Center of Materials and Nanotechnologies, Faculty of Chemical Technology, University of Pardubice, Nam. Cs. Legii, 530 02, 532 10 Pardubice, Czech Republic. E-mail: Jan.Macak@upce.cz; Tel: +420 466 037 401*
[c] *Central European Institute of Technology, Brno University of Technology, Purkynova 123, 612 00 Brno, Czech Republic*
[d] *Department of Physical Chemistry, Faculty of Chemical Technology, University of Pardubice, Studentska 573, 532 10 Pardubice, Czech Republic*
† Electronic supplementary information (ESI) available: SEM, dehydrogenase activity, glutathione levels. See DOI: https://doi.org/10.1039/d2en00217e
‡ Present address: Department of Inorganic Chemistry, Faculty of Natural Sciences, Comenius University in Bratislava, 842 15 Bratislava, Slovak Republic.

determine their potential cytotoxicity. The number of scientific reports on nanomaterial toxicity has rapidly increased over the last years.[7–11] The biological effects and toxicity of nanomaterials depend on their physicochemical properties, size, shape, purity, agglomeration, solubility, hydrophobic properties, surface charge and surface functionalization.[2,8,12–17] Due to their high reactivity, nanomaterials may induce specific cellular reactions that can lead to various types of toxicity.[18] However, the toxicity of a certain material is strongly dependent on its morphology and dimensionality. TiO_2 as an example can have different morphologies: nanoparticles (that tend to form agglomerates), nanofibers (that are rather separated and randomly oriented), anodic TiO_2 nanotubes (that are featured as layers of vertically aligned nanotubes), and some others. Even though they all have the same chemical composition, they might exhibit different levels of toxicity, as they possess diverse and morphologically related physicochemical properties.[17] As the worldwide intended and/or unintended exposure of living organisms to nanomaterials is increasing, it is crucial and relevant to study and evaluate the biological effects and toxicity of such materials on biological systems.[13,17]

The industrial environment enables the most common exposure of humans to nanomaterials and therefore it is the location possessing the highest potential health risk. Nanomaterials can usually enter the human body through the skin and the gastrointestinal or respiratory tract where the alveolar epithelial cells represent a major target of nanomaterials in the lungs. Thus, it is of high interest to test their pulmonary toxicity.[18–20] In general, the cell damage caused by nanomaterials leads to several pathological processes including apoptosis, necrosis, inflammation, fibrosis, hypertrophy, metaplasia, genotoxicity and/or carcinogenesis.[21] Moreover, the inhaled nanomaterials may increase the production of reactive oxygen species (ROS) and other oxidants in the human body and cause severe oxidative stress in the respiratory system.[22,23]

Nowadays technological advancements have enabled the synthesis of unique nanomaterials, including nanofibers. By definition, nanofibers should be fibers with a diameter lower than 100 nm, however, in the literature and especially in the textile industry, fibers with a diameter as large as 1 μm are still denoted as nanofibers (somewhat misleadingly). Nevertheless, the potential risk of nanofiber toxicity increases with growing worldwide production of different types of nanofibers despite no particular understanding of their toxicity. In addition, new technologies to produce nanofibers are being developed, including various versions of centrifugal spinning[24–26] with a little-to-no concern about the environmental impact of such materials. While centrifugal spinning and electrospinning can lead to nanofibers of comparable fiber diameter (some 50–800 nm), there are some distinct advantages of centrifugal spinning, as shown in our recent work.[27]

Regardless of the fiber technology used, the most common pathway where the nanofibers can permeate the human body is *via* inhalation to lungs.[20,28] Surprisingly, the *in vitro* cytotoxicity of nanofibers has not been sufficiently investigated in comparison to other nanomaterials such as nanoparticles,[21] nanotubes[16] or nanosheets.[28] Several recent studies investigated the biological effects of anatase TiO_2 nanofibers (obtained commercially or "home-made") mostly in pulmonary cells[8,12,19,29] and HeLa cells.[30] However, there is no study that would compare the biological effects of inorganic fibers of various chemical compositions that are entering the market. Studies focused on this topic are highly needed, thus, the aim of the present study is to determine the potential pulmonary toxicity *in vitro* of newly synthesized, commercially available SiO_2, TiO_2, Al_2O_3, ZrO_2 and WO_3 fibers (produced by centrifugal spinning) in frequently used human lung carcinoma epithelial A549 cells and to compare their potential biological effects with nanoparticles of the same chemical composition. Inorganic fibers investigated here are produced by centrifugal spinning into 3D cotton-like fluffy objects that are not suitable for further processing and commercial sale. Thus, in the production facility they are post-treated by milling, to become more homogeneous and powder-like, to be easily processed in all possible applications. Thus, the fibers in this work were investigated in the milled state to reflect the state in which they are sold. The main intention was to perform an introductory screening in cells to compare the biological effects of NPs and fibers of the same chemical composition.

Experimental

Materials used in this work

A summary of all types of samples used in this work is given in Table 1. The fibers were prepared by centrifugal spinning from suitable solutions and subsequent calcinations. They were all supplied by the company Pardam Nano4Fibers, Ltd., as samples that represent their standard portfolio for inorganic fibers. Since all these materials have no dimension below 100 nm, they are denoted as "fibers" in this work (to be aligned with the official EU nomenclature from the "Recommendation on the definition of a nanomaterial", 2011/696/EU), and not nanofibers, as common in some literature on centrifugal spinning and in the textile field. On the other hand, the reference materials (inorganic nanoparticles and multi-walled carbon nanotubes, MWCNTs) have their particle/tube diameter below 100 nm, so the term "nanoparticle" or "nanotube" is correct. There are no reference nanofibers with an average diameter below 100 nm that could be used for this work and presented comparison.

All fibers used in this work were synthesized according to the protocol described in our recent work on SiO_2 and WO_3 fibers.[26,31] The TiO_2, Al_2O_3, ZrO_2 and WO_3 fibers were prepared exactly the same way and instrumentation, but using titanium *tert*-butoxide for TiO_2, aluminium propoxide for Al_2O_3, zirconium *tert*-butoxide for ZrO_2, and ammonium

Table 1 Overview of the materials used in this work

Type of nanomaterial	Commercial name	Abbreviation used in this work	Origin
Fibers	Fiber CERAM – SiO_2 sorbent	SiO_2 sorbent	Pardam Nano4Fibers
	Fiber CERAM – SiO_2 Vs	SiO_2 VS	Pardam Nano4Fibers
	Fiber CERAM – Al_2O_3 α	Al_2O_3 α	Pardam Nano4Fibers
	Fiber CERAM – Al_2O_3 γ	Al_2O_3 γ	Pardam Nano4Fibers
	Fiber CERAM – TiO_2 rutile	TiO_2 rutile	Pardam Nano4Fibers
	Fiber CERAM – ZrO_2	ZrO_2	Pardam Nano4Fibers
	Fiber WO_3	WO_3	Pardam Nano4Fibers
Nanoparticles	SiO_2 nanoparticles (JRCNM02002a)	SiO_2 NP	JRC Nanomaterials Repository
	Al_2O_3 nanoparticles (544833)	Al_2O_3 NP	Sigma-Aldrich
	TiO_2 P25 nanoparticles	TiO_2 P25	Evonik Degussa
	ZrO_2 nanoparticles (544760)	ZrO_2 NP	Sigma-Aldrich
	WO_3 nanoparticles (550086)	WO_3 NP	Sigma-Aldrich
Nanotubes	Multi-walled carbon nanotubes (JRCNM40003a)	MWCNT	JRC Nanomaterials Repository

metatungstate for WO_3 respectively. More details about the principle of the centrifugal spinning and processes towards inorganic fibers can be obtained elsewhere.[24–26,31]

The resulting inorganic fibers, named "as-prepared" fibers in this work, kept their 3D bulky character, which was not suitable for the cell experiments. Thus, it was necessary to shorten the resulting fibers *via* ball milling using a spherical mill (Retsch) with the use of an agate milling container with a volume of 500 ml and agate milling balls of 10 mm in diameter. The ball-milled fibers, named "ball-milled" fibers in this work, were significantly shortened, but kept their fiber shape. Moreover, they became powder-like, which was more suitable for further handling (weighing, dispersing in water, exposure to cell lines, *etc.*). Al_2O_3, ZrO_2 and TiO_2 P25 nanoparticles were supplied by Sigma-Aldrich. SiO_2 nanoparticles and multiwalled carbon nanotubes (MWCNTs) were obtained from the JRC Nanomaterials Repository.

Characterization of nanomaterials

The morphological characterization of the calcined inorganic fibers, the ball-milled fibers and all other reference materials used in this work (Table 1) was carried out using a field-emission scanning electron microscope (FE-SEM, JSM7500F, JEOL). Energy-dispersive X-ray spectroscopy (EDX) was used to analyze the composition of the samples using an EDX detector (Oxford Instruments) integrated in a SEM (TESCAN MIRA3-XMU) by employing an accelerating voltage of 20 kV. The crystalline structure of the ball-milled fibers was characterized using an X-ray diffractometer (XRD, PANalytical Empyrean Cu Kα radiation, λ = 1.5418 Å) with a scintillation detector Pixcel^{3D} in the 2θ range 5–65°, the step size was 0.026°. The textural properties (specific surface area and pore size distribution) of the ball-milled fibers were determined from the N_2 adsorption isotherms. The isotherms were acquired using an ASAP 2020 instrument (Micromeritics) and evaluated with MicroActive Software (Micromeritics). The specific surface area was calculated according to the Brunauer–Emmett–Teller (BET) method.[32] The mesopore and external surface area, as well as the micropore volume, were determined by means of *t*-plot using the Harkins–Jura equation for calculation of the adsorbed layer thickness on oxidic materials and the "carbon black STSA" thickness curve equation for the MWCNT material. The pore volume and pore size distribution were determined by the NL DFT approach by using the "N_2@77 K-cylindrical pore and oxide surface" kernel for oxidic materials and the "N_2@77 K carbon cylindrical pore MWNT" kernel for the MWCNT material.

Estimation of fibers' effects in cells

Endotoxin contamination. Powder materials were suspended in endotoxin-free water and diluted at a concentration of 1 mg mL^{-1}. All samples were vigorously vortexed and sonicated for 15 min. Then, the samples were centrifuged at 15 000 *g* for 15 min. The endotoxin concentration was measured in the supernatant using the PyroGene™ recombinant factor C assay (Lonza, Blackley, UK). According to the manufacturer's instructions, the presence of endotoxin in a sample was calculated using the standard curve and results were expressed as the endotoxin concentration in EU mL^{-1}.

Cells and cell culture. The human lung carcinoma epithelial cell line (A549, ATCC CCL-185, Manassas, VA, USA) was derived from human lung adenocarcinoma cells.[33] The cells were cultured in minimum essential medium (MEM, Invitrogen-Gibco, USA) supplemented with 10% (v/v) fetal bovine serum (FBS, Invitrogen-Gibco, USA), 2 mmol L^{-1} glutamine (Invitrogen-Gibco, USA), 1 mmol L^{-1} pyruvate (Invitrogen-Gibco, USA), 10 mmol L^{-1} HEPES (Invitrogen-Gibco, USA), and 50 μmol L^{-1} penicillin–streptomycin solution (Invitrogen-Gibco, USA) and maintained at 37 °C in a sterile humidified atmosphere of 5% CO_2. Exposure was initiated at 70% cell confluence. The cells were proven to be mycoplasma-free and the origin of the cells was confirmed by short tandem repeat analysis.

Cell treatment. The tested materials (*i.e.*, nanoparticles and fibers) were suspended in medium with 10% FBS to prepare the stock solutions at a concentration 1 mg mL^{-1}. After sonication in an ultrasonic bath K2 (60 J s^{-1}, 33 kHz, Kraintek, Slovakia) for 10 min to ensure a substantial dispersion, the working solutions were prepared by dilution

in the culture medium with 10% FBS to final concentrations (1, 10 and 100 μg mL^{-1}). We used FBS to sustain the colloidal stability of dispersed materials in the presence of serum proteins similarly to plasmatic proteins in human extracellular fluids. A549 cells were seeded into 96-well plates at a density of 5×10^3 cells per well. After 24 h of seeding, the cells were exposed to the materials. Before addition of the tested materials to the cells, all working solutions were thoroughly mixed and then added to the A549 cells. The cells were incubated with materials for 24 or 48 h and the biological effect was tested. Untreated cells were used as a negative control. The multiwalled carbon nanotubes (MWCNTs, JRC Nanomaterials Repository, Ispra, Varese, Italy) at a concentration of 100 μg mL^{-1} (*i.e.* 31 μg cm^{-2} in a well of 96-well plates) were established as a positive control.

Cell viability testing. The cell viability was assessed using the WST-1 test (Sigma-Aldrich, USA). The WST-1 test detects the activity of intracellular dehydrogenases. After the treatment, the cells were incubated with the WST-1 reagent according to the manufacturer's instructions for 1 h. The change of absorbance was measured using a spectrophotometer at a wavelength of 440 nm using a SPARK microplate reader (Tecan, Austria) while incubated at 37 °C. The dehydrogenase activity was expressed as the percentage of total cellular dehydrogenase activity relative to that in control cells (control = 100%).

Measurement of glutathione levels. The glutathione (GSH) levels were measured using an optimized bimane assay.[34] The working solutions of monochlorobimane (MCB, Sigma-Aldrich, USA) were prepared fresh at the time of analysis by dilution in Dulbecco's phosphate buffer (pH 7; 1 mmol L^{-1}, Sigma-Aldrich, USA) and tempered at 37 °C for 30 min. After the treatment of cells with the tested materials, 20 μL of the MCB solution was added to the cells in 96-well plates and the measurement started immediately (final concentration of MCB in a well was 40 μmol L^{-1}). The fluorescence intensity (E_x = 394 nm; E_m = 490 nm) was measured kinetically for 20 min using a SPARK microplate reader (Tecan, Austria). The fluorescence was expressed as the slope of a fluorescence change over time. The GSH levels were expressed as the percentage relative to the GSH levels in control cells (control = 100%).

In addition, we evaluated the occurrence of interference of materials with the WST-1 and GSH assays. At the tested concentrations, no significant interference of materials with any of the used assays was found. The background signal was always less than 5% of that in negative controls.

Statistical analysis. All experiments were repeated at least three times independently. Three replicates were used in each independent experiment. The results are expressed as a mean ± S.D. Statistical analysis was performed using OriginPro 9.0.0 (OriginLab, USA). The analysis of variance followed by Tukey's post-test was used to perform the mean comparison at a significance level $P = 0.05$ (*, $P < 0.05$, **, $P < 0.01$, ***, $P < 0.001$).

Results and discussion

Characterization of fibers

The as-spun fibers were calcined to remove the carbonaceous compounds (*i.e.*, carrier polymers and organic ligands of metal–organic precursors). Therefore, the fibers experienced some volume contraction and gravimetric loss based on the burn-out of these compounds. However, the structural integrity and the 3D bulky character of the fibers were preserved after calcination. This is well supported by the SEM images in Fig. 1 that show the as-prepared fibers. The SEM images of the same materials, but at higher magnification are shown in Fig. S1.†

Fig. 2 shows the SEM images of the corresponding ball-milled inorganic fibers as a result of milling of the same fibers shown in Fig. 1. As one can see from these images, the fibers did not crack longitudinally (along their bodies), but across their bodies. So, at the end, they became shorter than the as-produced fibers shown in Fig. 1 and S1,† but not necessarily smaller in diameter. Some fibers (*e.g.* TiO_2, ZrO_2, SiO_2 VS) survived the milling without any further morphological change apart from shortening, as demonstrated for these selected fiber examples in Fig. S2.† However, some other fibers underwent also partial disintegration to nanoparticles (small fraction though) on the side of the fibers, such as the SiO_2 sorbent and WO_3 fibers. For these fibers, according to Fig. 2, there are clearly broken fiber fragments embedded in the network of agglomerated nanoparticles, most likely due to their amorphous nature and overall brittleness. Fig. S3† shows the reference nanomaterials used in this work in the as-purchased state.

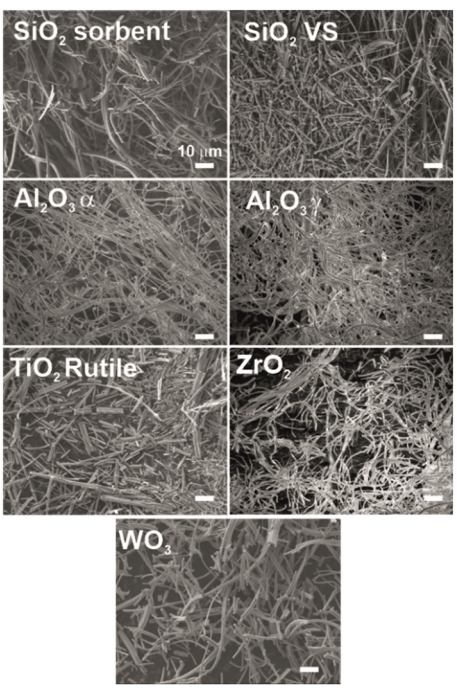

Fig. 1 SEM images of the as-prepared inorganic fibers (scale bars represent 10 μm).

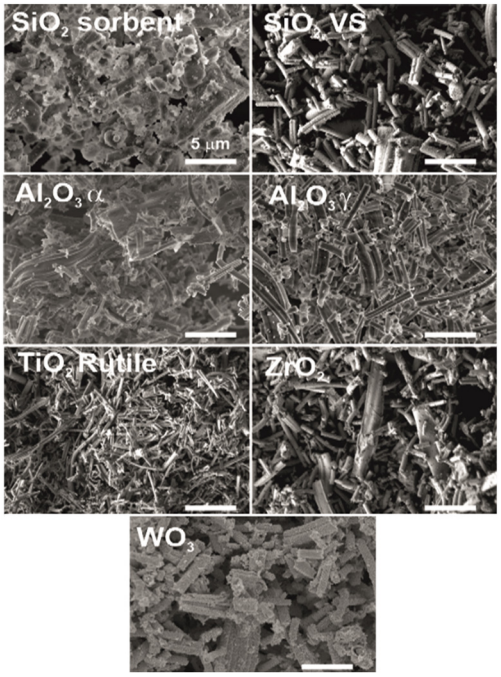

Fig. 2 SEM images of the ball-milled inorganic fibers used in this work for biological testing (scale bars represent 5 μm).

These nanomaterials were not anyhow ball-milled for the cell test. Statistical analyses of the fiber diameters and lengths (upon ball-milling) were carried out for all inorganic fibers shown in Fig. 2 as well as for the reference materials shown in Fig. S3.† The mean values and standard deviations are given in Table 2. As one can see, the average (mean) diameter of all fibers is on the scale of a few hundreds of nanometers, with a relatively broad diameter distribution. As one can see from these results, ball-milling results in fibers with an average length on the scale of 1.5 to 2.6 μm for all types of fibers, having a relatively broad distribution. Statistical analyses of the reference nanomaterials were carried out as well. The corresponding results are also shown in Table 2. All nanoparticles and MWCNTs have dimensions that fit with the product information.

Table 2 includes the elemental composition of the fibers obtained by EDX measurements. All fiber samples contained the expected elements. In general, the atomic percentage of the elements present in each sample correlates well with their respective composition.

The textural characterization of fibers, represented by BET analyses of the ball-milled fibers, showed that the highest total specific surface area was obtained in the case of SiO_2 fibers, as shown in Table 3. These fibers had also the largest diameter (d = 631 nm), as shown in Table 2, and the second largest volume of pores (V_{tot} = 0.342 m^3 g^{-1}), which is, together with the textural porosity, an essential parameter for any material to be a robust sorbent, able to capture water or other species, such as heavy metals.[26]

Fig. 3 shows the X-ray diffractograms of the fibers with crystalline structure. For the Al_2O_3 samples, a distinct single phase was revealed in both alpha and gamma cases. On the other hand, two phases were revealed in ZrO_2 fibers and both TiO_2 materials. However, it is typical for these materials to possess a multi-phase structure, in particular for materials calcined at a temperature of 500 °C. Nevertheless, TiO_2 fibers contained mostly the rutile phase (and only a minor anatase content). Last but not least, both types of SiO_2 fibers were amorphous, yielding only a typical broad diffraction pattern (shown in Fig. S4†), which is in line with our previous work.[26] Fig. S5† shows the X-ray diffractograms of the reference nanoparticles and MWCNTs for comparison. In fact, most of the reference materials, including MWCNTs, were crystalline, except SiO_2 nanoparticles, which were amorphous as well as their fiber counterparts (as shown in Fig. S4†).

The effect of fibers and reference materials in pulmonary A549 cells

Cellular dehydrogenase activity. The aim of our study was to evaluate the biological effects of various materials differing in their shape and chemical composition. We chose lung A549 cells which were treated with all tested materials shown in Table 1 for 24 and 48 h. The tested concentrations were 1,

Table 2 Statistical evaluation of diameters and lengths of the fibers shown in Fig. 2 and diameters of the nanoparticles shown in Fig. S2†

Samples	Mean diameter (nm)	Standard deviation (nm)	Mean length (nm)	Standard deviation (nm)	Elements revealed by EDX (atomic%)
SiO_2 sorbent	631	236	2167	1291	Si 27.83/O 72.17
SiO_2 VS	509	172	2063	1002	Si 34.44/O 65.66
Al_2O_3 α	392	152	2611	1738	Al 40.57/O 59.43
Al_2O_3 γ	496	128	2007	1683	Al 40.1/O 59.9
TiO_2 rutile	219	69	1597	1386	Ti 27.21/O 72.79
ZrO_2	432	85	2166	1510	Zr 29.71/O 70.29
WO_3	1074	264	2410	1041	W 31.14/O 68.86
SiO_2 NP	15	5	N/A	N/A	Si 30.51/O 69.49
Al_2O_3 NP	65	26	N/A	N/A	Al 34.78/O 65.22
TiO_2 P25	20	8	N/A	N/A	Ti 35.24/O 64.76
ZrO_2 NP	30	11	N/A	N/A	Zr 32.38/O 67.62
WO_3 NP	66	48	N/A	N/A	W 40.09/O 59.91
MWCNT	13	3	N/A	N/A	C 94.94/O 5.06

Table 3 Textural properties of the ball-milled inorganic fibers and reference materials

Sample	S_{BET} ($m^2\ g^{-1}$)	$S_{meso+ext}$ ($m^2\ g^{-1}$)	V_μ ($cm^3\ g^{-1}$)	V_{tot} ($m^2\ g^{-1}$)	Characteristics
SiO_2 sorbent	460.0	387.3	0.031	0.342	Mesoporous material, pores between 2 and 10 nm
SiO_2 VS	96.5	92.6	0.002	0.417	Mesoporous material – pores are larger than 10 nm, broad distribution to 100 nm (or dinitrogen condensation in inter-particle void space)
Al_2O_3 α	5.2	5.2	0.000	0.015	No micro- and mesopores
Al_2O_3 γ	70.8	70.8	0.000	0.120	Small volume of pores below 10 nm
TiO_2 rutile	6.0	6.0	0.000	0.018	No micro- and mesopores
ZrO_2	8.9	8.9	0.000	0.032	No micro- and mesopores
WO_3	22.3	22.3	0.000	0.084	No micro- and mesopores
SiO_2 NPs	190	175.8	0.005	0.335	Non-porous material with a particle size (based on a geometric model of spherical particles) of 7.2 nm in radius, the total pore volume is related to the interparticle space
Al_2O_3 NPs	170	163.3	0.001	0.637	Non-porous material with a particle size (based on a geometric model of spherical particles) of 5.0 nm in radius, the total pore volume is related to the interparticle space
TiO_2 P25	54.8	48.8	0.002	0.142	Non-porous material, the radius is roughly estimated to be 12 nm (spherical particle). V_{tot} is related to condensation in inter-particle void space
ZrO_2 NPs	24	23.8	0.000	0.071	Non-porous material, with a particle size (based on a geometric model of spherical particles) of 21.8 nm in radius
WO_3 NPs	6.4	6.4	0.000	0.034	Non-porous material, with a particle size (based on a geometric model of spherical particles) of 65.4 nm in radius
MWCNTs	167.8	164.3	0.002	0.530	Steadily increasing adsorbed amount at higher relative pressure can be ascribed to the dinitrogen condensation in the inner void space of nanotubes (main part of the volume is related to the void space diameter above 20 nm)

10 and 100 μg mL^{-1}. In addition, MWCNTs inducing strong cell damage were used as a positive control.

Firstly, we estimated all tested materials for the endotoxin contamination. We found that the concentration of endotoxin in all fibers, nanoparticles and MWCNTs occurred at the detection limit of the assay (<0.005 EU mL^{-1}). Thus, all tested nanomaterials were proven to be endotoxin-free.

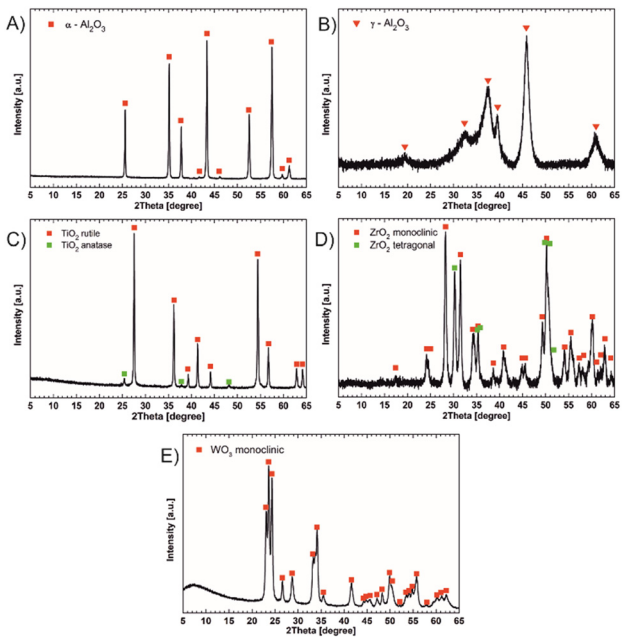

Fig. 3 X-ray diffractograms of the crystalline inorganic fibers: A) Al_2O_3 α, B) Al_2O_3 γ, C) TiO_2 rutile, D) ZrO_2, and E) WO_3.

Then, we estimated the effect of the materials on the cell viability by measurement of intracellular dehydrogenase activity using the WST-1 test. Our results (Fig. 4A) showed that 1 and 10 μg mL^{-1} concentrations of all tested materials except 10 μg mL^{-1} WO_3 did not induce a significant decrease in cellular dehydrogenase activity after 24 h of incubation. On the other hand, 24 h of treatment with 100 μg mL^{-1} Al_2O_3 α, TiO_2 rutile or WO_3 fibers and 100 μg mL^{-1} Al_2O_3, TiO_2 P25 or WO_3 NPs caused a significant decrease in dehydrogenase activity. The largest impairment was found in MWCNT and Al_2O_3 α fiber treated A549 cells, where the dehydrogenase activity was reduced to 73 ± 5% ($P < 0.001$) and 83 ± 7% ($P < 0.001$), respectively, compared to untreated cells.

After 48 h, we found that the cell damage predominantly deepened (Fig. 4A) in cells treated with 100 μg mL^{-1} concentration of some materials in comparison to 24 h. In addition, we detected a significant impairment in cells exposed also to 10 μg mL^{-1} SiO_2 VS fibers. Although the significant cell damage was induced by most of the tested materials, none of them caused cellular impairment at the extent comparable to MWCNTs. We conclude that according to the outcomes from the WST-1 test, the largest cellular impairment was caused by Al_2O_3- and TiO_2-derived materials. However, the cell damage was predominantly detectable only at the highest tested concentration and none of the tested materials induced cell damage comparable to MWCNTs. No significant changes of cell metabolism were observed in A549 cells treated with ZrO_2-derived materials. Importantly, no significant difference in induction of cell impairment was found after comparison of dehydrogenase activities of cells treated with fibers and NPs of the same chemical

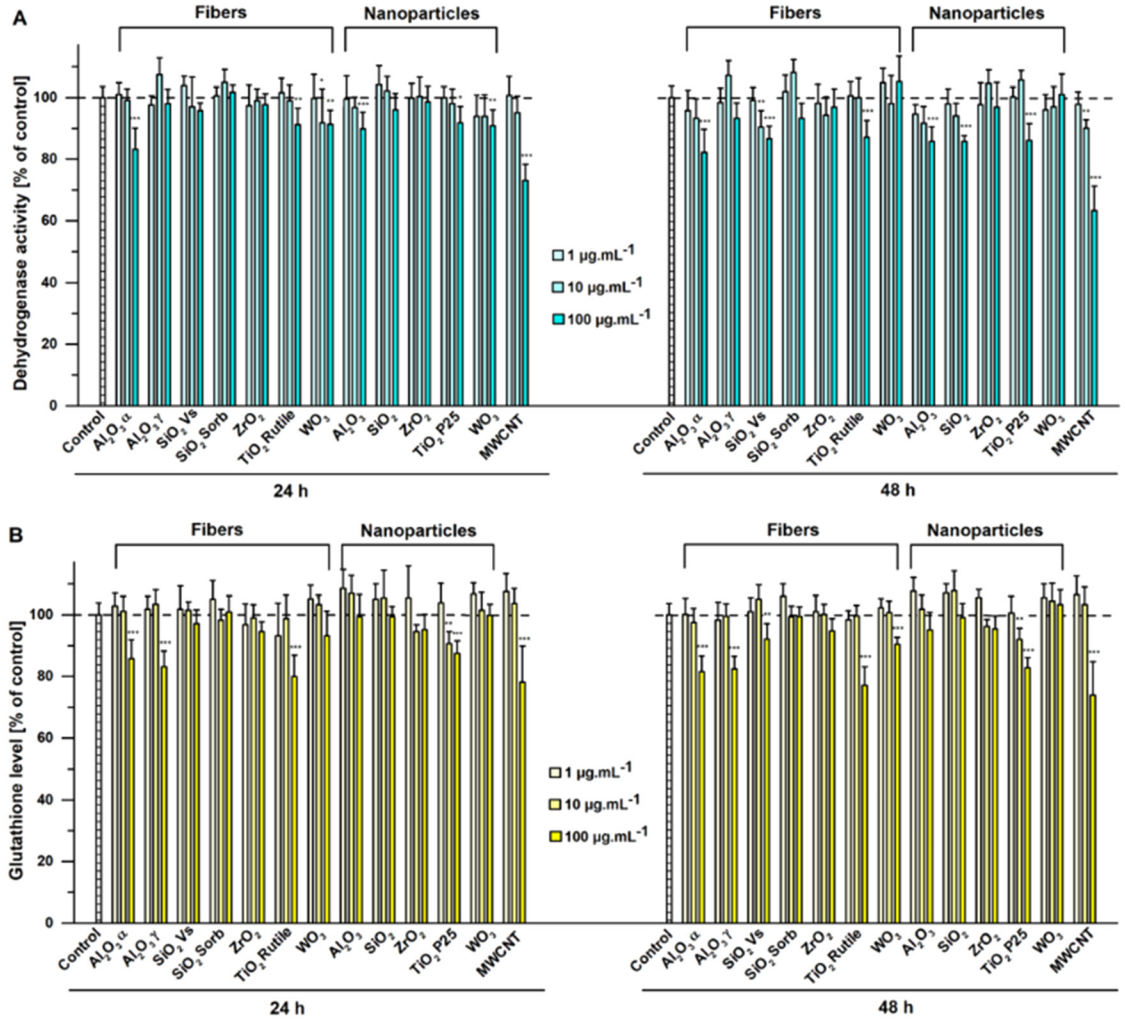

Fig. 4 Effect of the fibers and nanoparticles on the dehydrogenase activity (A) and glutathione levels (B) in A549 cells after 24 and 48 h of treatment. Data are expressed as mean ± SD (n = 12). *, $P < 0.05$, **, $P < 0.01$, ***, $P < 0.001$ *vs.* untreated control cells.

composition (the original data are reported in the ESI,† Table S1). Another graphical representation of the same results is shown for comparison in Fig. S6a,† where the grouping was carried out according to chemical compositions, not morphologies.

Glutathione levels. In addition to the WST-1 test, we measured the cellular levels of glutathione (GSH), as the essential intracellular antioxidant. The results on GSH levels (Fig. 4B) showed that there was a positive correlation with the findings observed using the WST-1 test. After 24 h of treatment, a significant glutathione depletion was found in A549 cells treated with 100 µg mL^{-1} Al_2O_3 α, Al_2O_3 γ and TiO_2 rutile fibers and with 100 µg mL^{-1} TiO_2 P25 in comparison with untreated cells. The largest GSH depletion was found in MWCNTs and TiO_2 rutile fibers treated cells where GSH levels were reduced to 78 ± 12% ($p < 0.001$) and 80 ± 7% ($p < 0.001$), respectively, compared to untreated cells. At 24 h, no significant effect on GSH levels was observed after treatment with SiO_2, ZrO_2 or WO_3 fibers and with Al_2O_3, SiO_2, ZrO_2 or WO_3 NPs.

After 48 h of treatment, GSH levels remained depleted in A549 cells treated with all materials causing GSH depletion after 24 h (Fig. 4B). In addition, significant GSH depletion was detected in A549 cells exposed to 100 µg mL^{-1} SiO_2 VS and WO_3 fibers. Although significant, the negative biological effect of SiO_2 VS and WO_3 fibers was, however, very mild because the incubation with both materials reduced the GSH levels only by 10%, compared to untreated cells. The largest GSH depletion was found again in MWCNT treated A549 cells (74 ± 11%, $p < 0.001$, *vs.* untreated cells). The GSH concentration after incubation with 100 µg mL^{-1} Al_2O_3 α, Al_2O_3 γ and TiO_2 rutile fibers or with 100 µg mL^{-1} TiO_2 P25 NPs occurred between 77% and 83% of GSH levels found in untreated cells. In summary and in accordance with the outcomes from the WST-1 test, the measurements of GSH levels in A549 cells treated with the tested materials did not show any significant relation of observed toxicity to the shape of a nanomaterial at similar concentrations. Only Al_2O_3 and WO_3 fibers at the highest concentration of 100 µg mL^{-1} seemed to exhibit a larger capability to deplete glutathione

levels than nanoparticles of the same chemical composition (the original data are reported in the ESI,† Table S2).

Another graphical representation of the same results is shown for comparison in Fig. S6b,† where the grouping was carried out according to chemical compositions, not morphologies.

Comprehensive discussion. A continuously increasing number of commercial products used in everyday life contain a considerable number of nanomaterials. The industrial environment causes the most common exposure of humans to nanomaterials and therefore it represents the largest potential health risk. The topical aim of the present study was to evaluate the cellular effects of new, unique types of inorganic fibers (Al_2O_3, SiO_2, ZrO_2, TiO_2 and WO_3). The biological effects of fibers were compared to commercially available Al_2O_3, SiO_2, ZrO_2, TiO_2 and WO_3 nanoparticles and MWCNTs. Our original intention was to perform an introductory screening in cells to compare the biological effects of NPs and fibers of the same chemical composition.

The toxicity of inorganic fibers depends on numerous factors such as chemical composition, length, persistency in the biological environment, dosage, mechanical resistance and solubility.[35] In general, penetration of a material (such as herein the presented fibers) into a living organism always depends on its dimensions and morphology and it is a complex process. An important factor that determines the toxicity of fiber materials, including asbestos, wires, tubes and fibers, are the length, aspect ratio and material structural changes,[8,36,37] which was confirmed by other studies providing a risk assessment of fibers.[38] There are studies reporting that for some materials (*e.g.*, carbon nanotubes,[39] ZnO nanoparticles[40]) the morphology and aspect ratio had an effect on the toxicity of particles and fibers.[41] We are convinced that our discussion on the effect of morphology and aspect ratio on toxicity will widen the current view in this field.

In general, all materials can be contaminated with endotoxins, *i.e.* lipopolysaccharides, during the manufacturing process, ball milling or handling. Endotoxin contamination of materials can report false positive results, including synergic pro-inflammatory effects and reactive oxygen species production.[42,43] Thus, we estimated all tested materials for endotoxin contamination. We confirmed that all tested materials were endotoxin-free, thus, they could be used for relevant biological testing in A549 cells.

The A549 human lung adenocarcinoma cell line was established in 1972.[44] It possesses characteristic features of the type II lung cells with typical lamellar bodies and consistent metabolic and transport properties.[33] Numerous toxicology studies reported the use of A549 lung cells in biological testing of nanomaterials including TiO_2, Ag_2O and ZrO_2 nanoparticles,[45–47] core–shell materials,[48] nanotubes,[49] nanowires[50] and nanosheets.[28] Because no information have been published on the relevant doses of nanomaterials during pulmonary exposure in humans, we selected the concentrations of the tested nanomaterials to be 1–100 μg mL^{-1} according to reports on the testing of viability and toxicity in cells after treatment with nanomaterials.[46,50–55]

We tested the treatment of A549 cells with fibers and nanoparticles in the range of concentrations 1–100 μg mL^{-1} for 24 and 48 h. We estimated the effects of nanomaterials on cell viability (*i.e.* intra- and extramitochondrial dehydrogenase activity measured using the WST-1 test) and intracellular GSH levels. We chose these two assays because the mitochondria can be an intracellular target of nanomaterials due to their reaction with highly reactive groups of mitochondrial proteins.[14,15] In addition, nanomaterials produce ROS causing oxidative stress.[56] The amount of generated ROS is dependent on the crystalline phase of the nanomaterial.[57] Moreover, because GSH is an important intracellular antioxidant acting as an electron donor,[21] the oxidative damage of cells can be monitored by measuring GSH depletion.[58] We used MWCNTs as a positive benchmark material for cell viability and GSH level evaluation. MWCNTs have been used as a reference positive control in a number of recent studies.[8,12,59–61] After 24 and 48 h, the treatments with 100 μg mL^{-1} MWCNTs reduced the cell viability and GSH levels approximately to 70% (compared to untreated cells). Other reports showed that 80 μg mL^{-1} MWCNTs significantly decreased the viability of A549 cells after 48 h.[62] In addition, MWCNTs were proven to have toxic effects on A549 cells after 24–72 h (ref. 8) and on alveolar macrophages after 1–5 days.[63] In summary, the susceptibility of A549 used in our study was comparable to other studies estimating MWCNT nanotoxicity.

Because of the uniqueness of the fibers tested in our study, we were not able to compare our outcomes with the results of experiments on testing fibers reported previously. Therefore, with our best effort, we compared our results on fiber toxicity assessment with other studies testing nanoparticles of the same chemical composition.

According to our results, the group of Al_2O_3-derived materials exhibited the largest toxicity. Although no toxicity was observed at concentrations 1 and 10 μg mL^{-1} in all tested Al_2O_3 fibers and NPs, we found a decrease in cell viability in A549 cells treated with 100 μg mL^{-1} Al_2O_3 α fibers and Al_2O_3 NPs. The changes of GSH levels confirmed the finding that 100 μg mL^{-1} Al_2O_3 fibers induced toxicity in treated cells as well. Some previous studies reported that 10–200 μg mL^{-1} Al_2O_3 NPs are capable of inducing cell impairment after 24 h incubation in human skin and murine fibroblasts.[64] Another study also observed a dose-dependent toxic effect on cell viability and GSH levels in multiple cell lines after exposure to Al_2O_3 αand Al_2O_3 γ NPs.[23] The toxic effect of Al_2O_3 NPs was reported also in other studies[65,66] confirming our findings on the general toxicity of Al_2O_3 materials.

SiO_2 fibers and NPs were not capable of inducing any cell injury at 24 h based on the WST-1 test outcomes. Comparable results can be found in recent studies reporting no decrease in cell viability after A549 cell treatment with 10 μg mL^{-1} SiO_2 NPs for 24 h.[67] After 48 h, the cell viability was slightly decreased in 100 μg mL^{-1} SiO_2 VS fibers and SiO_2

NPs. Here the presented finding of the time-dependent toxic effect of incubation with SiO_2-derived materials can be supported by a study reporting toxicity in 100 μg mL^{-1} SiO_2 NPs treated cells for 48 h.[46] Further, some studies reported that SiO_2 NPs are capable of inducing GSH depletion at levels ≥50 μg mL^{-1} after 24 h (ref. 68 and 69) and 48 h of treatment.[70] Our results, however, showed that GSH levels were significantly decreased after incubation of A549 cells only with 100 μg mL^{-1} SiO_2 VS fibers at 48 h. The difference in the induction of glutathione depletion between the two types of SiO_2 fibers may be caused by the slightly different chemical composition, diameter or surface area of the fibers. However, it is difficult to quantify at this stage what contribution can be prevailing for this trend.

After treatment with ZrO_2 fibers, we found no biological effects on both dehydrogenase activity and glutathione levels in A549 cells. Only, at 48 h, the concentration of 100 μg mL^{-1} ZrO_2 fibers induced an insignificant GSH depletion. Despite a limited number of studies using ZrO_2 materials, our results showing negligible cellular effects of ZrO_2 fibers are in good accordance with studies of Brunner *et al.*[71] reporting good biocompatibility of ZrO_2 NPs, of Stoccoro *et al.*[72] evaluating the surface modification in ZrO_2 NPs and of Karunakaran *et al.*[73] reporting that a decrease in the cell viability can be observed only after treatment with ≥200 μg mL^{-1} ZrO_2 NPs for 48 h.

In our study, we also tested the biological effects of TiO_2 rutile fibers on A549 cells. We detected changes in intracellular dehydrogenase activity and GSH depletion in all incubation times with the highest concentration, *i.e.*, with 100 μg mL^{-1} TiO_2 rutile fibers. There is only a limited number of studies that addressed the toxic potential of modified TiO_2 materials, thus the results presented here can be compared only with studies using TiO_2 anatase fibers. Hamilton *et al.* (2009) showed that the change of an anatase TiO_2 nanomaterial to a fiber larger than 15 μm created highly toxic particles and caused inflammatory response by alveolar macrophages very similar to asbestos and silica fibers.[36] A recent paper concluded that the effect of TiO_2 fibers caused a cell-specific, dose-dependent decrease of cell viability, with larger effects on alveolar epithelial cells than on macrophages (Allegri *et al.*[12]). Similar reports revealed that fibers from TiO_2 anatase may induce a significant cytotoxicity likely caused by the ROS generation.[30] In the study by Bianchi *et al.*,[8] two different batches of TiO_2 fibers with different overall lengths were investigated. It was shown that longer TiO_2 fibers (corresponding to the batch with 50% of fibers longer than 15 μm) were more cytotoxic than shorter TiO_2 nanofibers (corresponding to the batch with 5% of fibers longer than 15 μm, the rest shorter).[8] In addition, the biological effects of the here tested fibers TiO_2 rutile were compared with the commercial NP TiO_2 P25 which have been widely used in the literature. We found a significant decrease of cell viability after 24 and 48 h of treatment with 100 μg mL^{-1} TiO_2 P25 in A549 cells and a significant GSH depletion after 24 and 48 h. This is in good agreement with a number of previous papers reporting similar findings of decreased cell viability and GSH depletion in the A549 cells after exposure to TiO_2 P25.[10,45,54,74–77]

The last group of tested materials consisted of WO_3. We tested WO_3 fibers and NPs causing a mild decrease in dehydrogenase activity only after 24 h because A549 cells recovered the dehydrogenase activity after 48 h. Our results can be compared only with a limited number of reports evaluating the biological effects of WO_3 NPs reporting that WO_3 NPs induced no significant cell damage after 24 h incubation with several cell lines.[10,45,54,74–80] Thus, our results are in accordance with those studies showing no significant toxicity of WO_3 derived materials.

Conclusions

In our study, we evaluated the cellular toxicity of unique inorganic fibers, which have been recently synthesized and brought to the market. We conclude that fibers seem to be equal or even less potent inducers of cell damage in comparison to nanoparticles of the same chemical composition. In addition, we found that the tested fibers of different chemical composition caused no or very mild cell impairment in pulmonary A549 cells treated only with the highest concentration, *i.e.*, 100 μg mL^{-1}. On the other hand, Al_2O_3 α and Al_2O_3 γ fibers were found to cause moderate cell toxicity generally implying their possible limitations for the use in biological applications. The present study on testing elementary biological effects of inorganic fibers and nanoparticles provides primary findings that can serve as a basis for further, more detailed scientific studies.

Author contributions

JB, TR and JMM designed the experiments; JB, PN, LB, TR performed the biological assessment of all nanomaterials; LH conducted milling of fibers; LH, MM, RB, MR performed physicochemical characterization and analyzed the data; JB, LH, TR, MM and JMM wrote the manuscript; all others reviewed and edited the manuscript; TR and JMM supervised the team and provided support. All authors have read and agreed to the published version of the manuscript.

Conflicts of interest

There are no conflicts to declare.

Acknowledgements

The authors acknowledge the financial support from the Ministry of Education, Youth and Sports of the Czech Republic (projects NANOBIO CZ.02.1.01/0.0/0.0/17_048/0007421 and LM2018103). EDX measurements were carried out with the support of CEITEC Nano Research Infrastructure (LM 2018110, MEYS CR, 2020–2022).

Notes and references

1 R. Bayford, T. Rademacher, I. Roitt and S. X. Wang, Emerging applications of nanotechnology for diagnosis and therapy of disease: a review, *Physiol. Meas.*, 2017, **38**, R183–R203.
2 A. J. Ferreira, J. Cemlyn-Jones and C. Robalo Cordeiro, Nanoparticles, nanotechnology and pulmonary nanotoxicology, *Rev. Port. Pneumol.*, 2013, **19**, 28–37.
3 R. Landsiedel, U. G. Sauer, L. Ma-Hock, J. Schnekenburger and M. Wiemann, *Nanomedicine*, 2014, **9**, 2557–2585.
4 D. A. Richards, A. Maruani and V. Chudasama, Antibody fragments as nanoparticle targeting ligands: a step in the right direction, *Chem. Sci.*, 2016, **8**, 63–77.
5 S. Panimalar, S. Logambal, R. Thambidurai, C. Inmozhi, R. Uthrakumar, A. Muthukumaran, R. A. Rasheed, M. K. Gatasheh, A. Raja, J. Kennedy and K. Kaviyarasu, Effect of Ag doped MnO2 nanostructures suitable for wastewater treatment and other environmental pollutant applications, *Environ. Res.*, 2022, **205**, 112560.
6 K. Kaviyarasu, N. Geetha, K. Kanimozhi, C. Maria Magdalane, S. Sivaranjani, A. Ayeshamariam, J. Kennedy and M. Maaza, In vitro cytotoxicity effect and antibacterial performance of human lung epithelial cells A549 activity of Zinc oxide doped TiO2 nanocrystals: Investigation of bio-medical application by chemical method, *Mater. Sci. Eng., C*, 2017, **74**, 325–333.
7 R. Bengalli, S. Ortelli, M. Blosi, A. Costa, P. Mantecca and L. Fiandra, In Vitro Toxicity of TiO2:SiO2 Nanocomposites with Different Photocatalytic Properties, *Nanomaterials*, 2019, **9**, 1041.
8 M. G. Bianchi, L. Campagnolo, M. Allegri, S. Ortelli, M. Blosi, M. Chiu, G. Taurino, V. Lacconi, A. Pietroiusti, A. L. Costa, C. A. Poland, D. Baird, R. Duffin, O. Bussolati and E. Bergamaschi, Length-dependent toxicity of TiO2 nanofibers: mitigation via shortening, *Nanotoxicology*, 2020, **14**, 433–452.
9 M. Dusinska, J. Tulinska, N. El Yamani, M. Kuricova, A. Liskova, E. Rollerova, E. Rundén-Pran and B. Smolkova, Immunotoxicity, genotoxicity and epigenetic toxicity of nanomaterials: New strategies for toxicity testing?, *Food Chem. Toxicol.*, 2017, **109**, 797–811.
10 C. L. Ursini, D. Cavallo, A. M. Fresegna, A. Ciervo, R. Maiello, P. Tassone, G. Buresti, S. Casciardi and S. Iavicoli, Evaluation of cytotoxic, genotoxic and inflammatory response in human alveolar and bronchial epithelial cells exposed to titanium dioxide nanoparticles, *J. Appl. Toxicol.*, 2014, **34**, 1209–1219.
11 N. El Yamani, A. R. Collins, E. Rundén-Pran, L. M. Fjellsbø, S. Shaposhnikov, S. Zielonddiny and M. Dusinska, In vitro genotoxicity testing of four reference metal nanomaterials, titanium dioxide, zinc oxide, cerium oxide and silver: towards reliable hazard assessment, *Mutagenesis*, 2017, **32**, 117–126.
12 M. Allegri, M. G. Bianchi, M. Chiu, J. Varet, A. L. Costa, S. Ortelli, M. Blosi, O. Bussolati, C. A. Poland and E. Bergamaschi, Shape-Related Toxicity of Titanium Dioxide Nanofibres, *PLoS One*, 2016, **11**, e0151365.
13 K. Bhattacharya, G. Kiliç, P. M. Costa and B. Fadeel, Cytotoxicity screening and cytokine profiling of nineteen nanomaterials enables hazard ranking and grouping based on inflammogenic potential, *Nanotoxicology*, 2017, **11**, 809–826.
14 A. Manke, L. Wang and Y. Rojanasakul, Mechanisms of Nanoparticle-Induced Oxidative Stress and Toxicity, *BioMed Res. Int.*, 2013, **2013**, 1–15.
15 A. Nel, T. Xia, L. Mädler and N. Li, *Science*, 2006, **311**, 622–627.
16 H. Michalkova, Z. Skubalova, H. Sopha, V. Strmiska, B. Tesarova, S. Dostalova, P. Svec, L. Hromadko, M. Motola, J. M. J. M. Macak, V. Adam and Z. Heger, Complex cytotoxicity mechanism of bundles formed from self-organised 1-D anodic TiO<inf>2</inf> nanotubes layers, *J. Hazard. Mater.*, 2020, **388**, 122054.
17 S. K. Sohaebuddin, P. T. Thevenot, D. Baker, J. W. Eaton and L. Tang, Nanomaterial cytotoxicity is composition, size, and cell type dependent, *Part. Fibre Toxicol.*, 2010, **7**, 1–17.
18 S. Arora, J. M. Rajwade and K. M. Paknikar, *Toxicol. Appl. Pharmacol.*, 2012, **258**, 151–165.
19 H. K. Lindberg, G. C. M. Falck, S. Suhonen, M. Vippola, E. Vanhala, J. Catalán, K. Savolainen and H. Norppa, Genotoxicity of nanomaterials: DNA damage and micronuclei induced by carbon nanotubes and graphite nanofibres in human bronchial epithelial cells in vitro, *Toxicol. Lett.*, 2009, **186**, 166–173.
20 P. A. Tran, L. Zhang and T. J. Webster, *Adv. Drug Delivery Rev.*, 2009, **61**, 1097–1114.
21 N. Lewinski, V. Colvin and R. Drezek, *Small*, 2008, **4**, 26–49.
22 T. Vlachogianni, K. Fiotakis, S. Loridas, S. Perdicaris and A. Valavanidis, *Lung Cancer: Targets Ther.*, 2013, **4**, 71–82.
23 E. J. Park, G. H. Lee, C. Yoon, U. Jeong, Y. Kim, M. H. Cho and D. W. Kim, Biodistribution and toxicity of spherical aluminum oxide nanoparticles, *J. Appl. Toxicol.*, 2016, **36**, 424–433.
24 K. Sarkar, C. Gomez, S. Zambrano, M. Ramirez, E. De Hoyos, H. Vasquez and K. Lozano, Electrospinning to Forcespinning™, *Mater. Today*, 2010, **13**, 12–14.
25 L. Ren, R. Ozisik and S. P. Kotha, Rapid and efficient fabrication of multilevel structured silica micro−/nanofibers by centrifugal jet spinning, *J. Colloid Interface Sci.*, 2014, **425**, 136–142.
26 L. Hromádko, E. Koudelková, R. Bulánek and J. M. Macak, SiO2 Fibers by Centrifugal Spinning with Excellent Textural Properties and Water Adsorption Performance, *ACS Omega*, 2017, **2**, 5052–5059.
27 M. Rihova, A. E. Ince, V. Cicmancova, L. Hromadko, K. Castkova, D. Pavlinak, L. Vojtova and J. M. Macak, Water-born 3D nanofiber mats using cost-effective centrifugal spinning: comparison with electrospinning process: A complex study, *J. Appl. Polym. Sci.*, 2021, **138**, 49975.

28 T. A. Tabish, M. Z. I. Pranjol, H. Hayat, A. A. M. Rahat, T. M. Abdullah, J. L. Whatmore and S. Zhang, In vitro toxic effects of reduced graphene oxide nanosheets on lung cancer cells, *Nanotechnology*, 2017, **28**, 504001.

29 E. I. Medina-Reyes, N. L. Delgado-Buenrostro, A. Déciga-Alcaraz, V. Freyre-Fonseca, J. O. Flores-Flores, R. Hernández-Pando, J. Barrios-Payán, J. C. Carrero, Y. Sánchez-Pérez, C. M. García-Cuéllar, F. Vaca-Paniagua and Y. I. Chirino, Titanium dioxide nanofibers induce angiogenic markers and genomic instability in lung cells leading to a highly dedifferentiated and fibrotic tumor formation in a xenograft model, *Environ. Sci.: Nano*, 2019, **6**, 286–304.

30 K. M. Ramkumar, C. Manjula, G. Gnanakumar, M. A. Kanjwal, T. V. Sekar, R. Paulmurugan and P. Rajaguru, Oxidative stress-mediated cytotoxicity and apoptosis induction by TiO 2 nanofibers in HeLa cells, *Eur. J. Pharm. Biopharm.*, 2012, **81**, 324–333.

31 L. Hromádko, M. Motola, V. Čičmancová, R. Bulánek and J. M. Macak, Facile synthesis of WO3 fibers via centrifugal spinning as an efficient UV- and VIS-light-driven photocatalyst, *Ceram. Int.*, 2021, **47**, 35361–35365.

32 S. Brunauer, P. H. Emmett and E. Teller, Adsorption of Gases in Multimolecular Layers, *J. Am. Chem. Soc.*, 1938, **60**, 309–319.

33 K. A. Foster, C. G. Oster, M. M. Mayer, M. L. Avery and K. L. Audus, Characterization of the A549 cell line as a type II pulmonary epithelial cell model for drug metabolism, *Exp. Cell Res.*, 1998, **243**, 359–366.

34 J. Čapek, M. Hauschke, L. Brůčková and T. Roušar, Comparison of glutathione levels measured using optimized monochlorobimane assay with those from ortho-phthalaldehyde assay in intact cells, *J. Pharmacol. Toxicol. Methods*, 2017, **88**, 40–45.

35 K. Donaldson and C. L. Tran, An introduction to the short-term toxicology of respirable industrial fibres, *Mutat. Res., Fundam. Mol. Mech. Mutagen.*, 2004, **553**, 5–9.

36 R. F. Hamilton, N. Wu, D. Porter, M. Buford, M. Wolfarth and A. Holian, Particle length-dependent titanium dioxide nanomaterials toxicity and bioactivity, *Part. Fibre Toxicol.*, 2009, **6**, 1–11.

37 C. A. Poland, R. Duffin, I. Kinloch, A. Maynard, W. A. H. Wallace, A. Seaton, V. Stone, S. Brown, W. MacNee and K. Donaldson, Carbon nanotubes introduced into the abdominal cavity of mice show asbestos-like pathogenicity in a pilot study, *Nat. Nanotechnol.*, 2008, **3**, 423–428.

38 A. Schinwald, F. A. Murphy, A. Prina-Mello, C. A. Poland, F. Byrne, D. Movia, J. R. Glass, J. C. Dickerson, D. A. Schultz, C. E. Jeffree, W. MacNee and K. Donaldson, The Threshold Length for Fiber-Induced Acute Pleural Inflammation: Shedding Light on the Early Events in Asbestos-Induced Mesothelioma, *Toxicol. Sci.*, 2012, **128**, 461–470.

39 H.-J. Eom, J.-S. Jeong and J. Choi, Effect of aspect ratio on the uptake and toxicity of hydroxylated-multi walled carbon nanotubes in the nematode, Caenorhabditis elegans, *Environ. Health Toxicol.*, 2015, **30**, e2015001.

40 M. Samei, M. H. Sarrafzadeh and M. A. Faramarzi, The impact of morphology and size of zinc oxide nanoparticles on its toxicity to the freshwater microalga, Raphidocelis subcapitata, *Environ. Sci. Pollut. Res.*, 2019, **26**, 2409–2420.

41 N. Kamal, A. H. Zaki, A. A. G. El-Shahawy, O. M. Sayed and S. I. El-Dek, Changing the morphology of one-dimensional titanate nanostructures affects its tissue distribution and toxicity, *Toxicol. Ind. Health*, 2020, **36**, 272–286.

42 S. Smulders, J.-P. Kaiser, S. Zuin, K. L. Van Landuyt, L. Golanski, J. Vanoirbeek, P. Wick and P. H. Hoet, Contamination of nanoparticles by endotoxin: evaluation of different test methods, *Part. Fibre Toxicol.*, 2012, **9**, 1–11.

43 L. Di Cristo, D. Movia, M. G. Bianchi, M. Allegri, B. M. Mohamed, A. P. Bell, C. Moore, S. Pinelli, K. Rasmussen, J. Riego-Sintes, A. Prina-Mello, O. Bussolati and E. Bergamaschi, Proinflammatory effects of pyrogenic and precipitated amorphous silica nanoparticles in innate immunity cells, *Toxicol. Sci.*, 2016, **150**, 40–53.

44 M. Lieber, G. Todaro, B. Smith, A. Szakal and W. Nelson-Rees, A continuous tumor-cell line from a human lung carcinoma with properties of type II alveolar epithelial cells, *Int. J. Cancer*, 1976, **17**, 62–70.

45 R. Guadagnini, K. Moreau, S. Hussain, F. Marano and S. Boland, Toxicity evaluation of engineered nanoparticles for medical applications using pulmonary epithelial cells, *Nanotoxicology*, 2015, **9**, 25–32.

46 I. Hansjosten, J. Rapp, L. Reiner, R. Vatter, S. Fritsch-Decker, R. Peravali, T. Palosaari, E. Joossens, K. Gerloff, P. Macko, M. Whelan, D. Gilliland, I. Ojea-Jimenez, M. P. Monopoli, L. Rocks, D. Garry, K. Dawson, P. J. F. Röttgermann, A. Murschhauser, J. O. Rädler, S. V. Y. Tang, P. Gooden, M. F. A. Belinga-Desaunay, A. O. Khan, S. Briffa, E. Guggenheim, A. Papadiamantis, I. Lynch, E. Valsami-Jones, S. Diabaté and C. Weiss, Microscopy-based high-throughput assays enable multi-parametric analysis to assess adverse effects of nanomaterials in various cell lines, *Arch. Toxicol.*, 2018, **92**, 633–649.

47 S. Lanone, F. Rogerieux, J. Geys, A. Dupont, E. Maillot-Marechal, J. Boczkowski, G. Lacroix and P. Hoet, Comparative toxicity of 24 manufactured nanoparticles in human alveolar epithelial and macrophage cell lines, *Part. Fibre Toxicol.*, 2009, **6**, 14.

48 T. Wang, Y. Liu and C. Wu, Effect of Paclitaxel-Mesoporous Silica Nanoparticles with a Core-Shell Structure on the Human Lung Cancer Cell Line A549, *Nanoscale Res. Lett.*, 2017, **12**, 1–8.

49 G. Visalli, M. P. Bertuccio, D. Iannazzo, A. Piperno, A. Pistone and A. di Pietro, Toxicological assessment of multi-walled carbon nanotubes on A549 human lung epithelial cells, *Toxicol. In Vitro*, 2015, **29**, 352–362.

50 A. Cacchioli, F. Ravanetti, R. Alinovi, S. Pinelli, F. Rossi, M. Negri, E. Bedogni, M. Campanini, M. Galetti, M. Goldoni, P. Lagonegro, R. Alfieri, F. Bigi and G. Salviati, Cytocompatibility and cellular internalization mechanisms of SiC/SiO 2 nanowires, *Nano Lett.*, 2014, **14**, 4368–4375.

51 L. Ren, K. Pashayi, H. R. Fard, S. P. Kotha, T. Borca-Tasciuc and R. Ozisik, Engineering the coefficient of thermal expansion and thermal conductivity of polymers filled with

high aspect ratio silica nanofibers, *Composites, Part B*, 2014, **58**, 228–234.

52 R. Y. Prasad, K. Wallace, K. M. Daniel, A. H. Tennant, R. M. Zucker, J. Strickland, K. Dreher, A. D. Kligerman, C. F. Blackman and D. M. Demarini, Effect of treatment media on the agglomeration of titanium dioxide nanoparticles: Impact on genotoxicity, cellular interaction, and cell cycle, *ACS Nano*, 2013, **7**, 1929–1942.

53 L. Bobyk, A. Tarantini, D. Beal, G. Veronesi, I. Kieffer, S. Motellier, E. Valsami-Jones, I. Lynch, P. H. Jouneau, K. Pernet-Gallay, C. Aude-Garcia, S. Sauvaigo, T. Douki, T. Rabilloud and M. Carriere, Toxicity and chemical transformation of silver nanoparticles in A549 lung cells: Dose-rate-dependent genotoxic impact, *Environ. Sci.: Nano*, 2021, **8**, 806–821.

54 I. L. Hsiao and Y. J. Huang, Effects of various physicochemical characteristics on the toxicities of ZnO and TiO2 nanoparticles toward human lung epithelial cells, *Sci. Total Environ.*, 2011, **409**, 1219–1228.

55 J. Bacova, P. Knotek, K. Kopecka, L. Hromadko, J. Capek, P. Nyvltova, L. Bruckova, L. Schröterova, B. Sestakova, J. Palarcik, M. Motola, D. Cizkova, A. Bezrouk, J. Handl, Z. Fiala, E. Rudolf, Z. Bilkova, J. M. Macak and T. Rousar, Evaluating the Use of TiO2 Nanoparticles for Toxicity Testing in Pulmonary A549 Cells, *Int. J. Nanomed.*, 2022, **17**, 4211–4225.

56 H. Yang, C. Liu, D. Yang, H. Zhang and Z. Xi, Comparative study of cytotoxicity, oxidative stress and genotoxicity induced by four typical nanomaterials: The role of particle size, shape and composition, *J. Appl. Toxicol.*, 2009, **29**, 69–78.

57 M. Rosales, T. Zoltan, C. Yadarola, E. Mosquera, F. Gracia and A. García, The influence of the morphology of 1D TiO2 nanostructures on photogeneration of reactive oxygen species and enhanced photocatalytic activity, *J. Mol. Liq.*, 2019, **281**, 59–69.

58 J. Čapek and T. Roušar, *Molecules*, 2021, **26**, 4710.

59 M. Abdelgied, A. M. El-Gazzar, D. B. Alexander, W. T. Alexander, T. Numano, M. Iigou, A. Naiki-Ito, H. Takase, K. A. Abdou, A. Hirose, Y. Taquahashi, J. Kanno, M. Abdelhamid, H. Tsuda and S. Takahashi, Pulmonary and pleural toxicity of potassium octatitanate fibers, rutile titanium dioxide nanoparticles, and MWCNT-7 in male Fischer 344 rats, *Arch. Toxicol.*, 2019, **93**, 909–920.

60 S. Funahashi, Y. Okazaki, D. Ito, A. Asakawa, H. Nagai, M. Tajima and S. Toyokuni, Asbestos and multi-walled carbon nanotubes generate distinct oxidative responses in inflammatory cells, *J. Clin. Biochem. Nutr.*, 2015, **56**, 111–117.

61 K. Rasmussen, J. Mast, P.-J. De Temmerman, E. Verleysen, N. Waegeneers, F. Van Steen, J. C. Pizzolon, L. De Temmerman, E. Van Doren, K. A. Jensen, R. Birkedal, M. Levin, S. H. Nielsen, V. Kofoed-Sørensen, Y. Kembouche, N. Thieriet, O. Spalla, C. Giuot, D. Rousset, O. Witschger, S. Bau, B. Bianchi, C. Motzkus, B. Shivachev, L. Dimowa, R. Nikolova, D. Nihtianova, M. Tarassov, O. Petrov, S. Bakardjieva, D. Gilliand, F. Pianella, G. Ceccone, V. Spampinato, G. Cotogno, P. Gibson, C. Gaillard and A. Mech, *Titanium dioxide, NM-100, NM-101, NM-102, NM-103, NM-104, NM-105*, Publications Office of the EU, 2014.

62 M. Allegri, D. K. Perivoliotis, M. G. Bianchi, M. Chiu, A. Pagliaro, M. A. Koklioti, A. F. A. Trompeta, E. Bergamaschi, O. Bussolati and C. A. Charitidis, Toxicity determinants of multi-walled carbon nanotubes: The relationship between functionalization and agglomeration, *Toxicol. Rep.*, 2016, **3**, 230–243.

63 S. Sweeney, D. Grandolfo, P. Ruenraroengsak and T. D. Tetley, Functional consequences for primary human alveolar macrophages following treatment with long, but not short, multiwalled carbon nanotubes, *Int. J. Nanomed.*, 2015, **10**, 3115–3129.

64 E. Radziun, J. Dudkiewicz Wilczyńska, I. Ksiazek, K. Nowak, E. L. Anuszewska, A. Kunicki, A. Olszyna and T. Zabkowski, Assessment of the cytotoxicity of aluminium oxide nanoparticles on selected mammalian cells, *Toxicol. In Vitro*, 2011, **25**, 1694–1700.

65 Z. Xiao Qiang, Y. Li Hong, T. Meng and P. Yue Pu, ZnO, TiO_2, SiO_2, and Al_2O_3 Nanoparticlesinduced Toxic Effects on Human Fetal Lung Fibroblasts*, *Biomed. Environ. Sci.*, 2011, **24**, 661–669.

66 F. Arul Prakash, G. J. Dushendra Babu, M. Lavanya, K. S. Vidhya and T. Devasena, Toxicity Studies of Aluminium Oxide Nanoparticles in Cell Lines, *International Journal of Nanotechnology and Application*, 2011, **5**, 99–107.

67 C. F. Lu, L. Z. Li, W. Zhou, J. Zhao, Y. M. Wang and S. Q. Peng, Silica nanoparticles and lead acetate co-exposure triggered synergistic cytotoxicity in A549 cells through potentiation of mitochondria-dependent apoptosis induction, *Environ. Toxicol. Pharmacol.*, 2017, **52**, 114–120.

68 I. Y. Kim, E. Joachim, H. Choi and K. Kim, Toxicity of silica nanoparticles depends on size, dose, and cell type, *Nanomedicine*, 2015, **11**, 1407–1416.

69 W. Lin, Y. W. Huang, X. D. Zhou and Y. Ma, In vitro toxicity of silica nanoparticles in human lung cancer cells, *Toxicol. Appl. Pharmacol.*, 2006, **217**, 252–259.

70 U. De Simone, L. Manzo, A. Profumo and T. Coccini, In vitro toxicity evaluation of engineered cadmium-coated silica nanoparticles on human pulmonary cells, *J. Toxicol.*, 2013, **2013**, 1–10.

71 T. J. Brunner, P. Wick, P. Manser, P. Spohn, R. N. Grass, L. K. Limbach, A. Bruinink and W. J. Stark, In vitro cytotoxicity of oxide nanoparticles: Comparison to asbestos, silica, and the effect of particle solubility, *Environ. Sci. Technol.*, 2006, **40**, 4374–4381.

72 A. Stoccoro, S. Di Bucchianico, C. Uboldi, F. Coppedè, J. Ponti, C. Placidi, M. Blosi, S. Ortelli, A. L. Costa and L. Migliore, A panel of in vitro tests to evaluate genotoxic and morphological neoplastic transformation potential on Balb/3T3 cells by pristine and remediated titania and zirconia nanoparticles, *Mutagenesis*, 2016, **31**, 511–529.

73 G. Karunakaran, R. Suriyaprabha, P. Manivasakan, R. Yuvakkumar, V. Rajendran and N. Kannan, Screening of in vitro cytotoxicity, antioxidant potential and bioactivity of nano- and micro-ZrO2 and -TiO2 particles, *Ecotoxicol. Environ. Saf.*, 2013, **93**, 191–197.

74 B. Ekstrand-Hammarström, C. M. Akfur, P. O. Andersson, C. Lejon, L. Österlund and A. Bucht, Human primary bronchial epithelial cells respond differently to titanium dioxide nanoparticles than the lung epithelial cell lines A549 and BEAS-2B, *Nanotoxicology*, 2012, **6**, 623–634.

75 R. K. Shukla, V. Sharma, A. K. Pandey, S. Singh, S. Sultana and A. Dhawan, ROS-mediated genotoxicity induced by titanium dioxide nanoparticles in human epidermal cells, *Toxicol. In Vitro*, 2011, **25**, 231–241.

76 E. Moschini, M. Gualtieri, M. Colombo, U. Fascio, M. Camatini and P. Mantecca, The modality of cell-particle interactions drives the toxicity of nanosized CuO and TiO2 in human alveolar epithelial cells, *Toxicol. Lett.*, 2013, **222**, 102–116.

77 E. J. Park, J. Yi, K. H. Chung, D. Y. Ryu, J. Choi and K. Park, Oxidative stress and apoptosis induced by titanium dioxide nanoparticles in cultured BEAS-2B cells, *Toxicol. Lett.*, 2008, **180**, 222–229.

78 M. Horie, K. Fujita, H. Kato, S. Endoh, K. Nishio, L. K. Komaba, A. Nakamura, A. Miyauchi, S. Kinugasa, Y. Hagihara, E. Niki, Y. Yoshida and H. Iwahashi, Association of the physical and chemical properties and the cytotoxicity of metal oxidenanoparticles: metal ion release, adsorption ability and specific surface area, *Metallomics*, 2012, **4**, 350–360.

79 A. Ivask, T. Titma, M. Visnapuu, H. Vija, A. Kakinen, M. Sihtmae, S. Pokhrel, L. Madler, M. Heinlaan, V. Kisand, R. Shimmo and A. Kahru, Toxicity of 11 Metal Oxide Nanoparticles to Three Mammalian Cell Types In Vitro, *Curr. Top. Med. Chem.*, 2015, **15**, 1914–1929.

80 B. Han, A. L. Popov, T. O. Shekunova, D. A. Kozlov, O. S. Ivanova, A. A. Rumyantsev, A. B. Shcherbakov, N. R. Popova, A. E. Baranchikov and V. K. Ivanov, Highly Crystalline WO 3 Nanoparticles Are Nontoxic to Stem Cells and Cancer Cells, *J. Nanomater.*, 2019, **2019**, 1–13.

